

## Manipulation of PBDT-DTNT:PCBM Photoactive Layers for Stability

### Increment by Core-Shell and Core-Mantle-Shell Supramolecules

Jing Pan<sup>a</sup>, Zhe Jia<sup>a</sup>, Yuhong Chang<sup>a</sup>, Yi Hu<sup>a</sup>, Guanghua Zhang<sup>b,1</sup>, Samira Agbolaghi<sup>c,2</sup>

<sup>a</sup> Department of Physics and Chemistry, Taiyuan University, Taiyuan, Shanxi,  
030000, China

<sup>b</sup> Department of Computer Science and Engineering, Taiyuan University, Taiyuan,  
Shanxi, 030000, China

<sup>c</sup> Chemical Engineering Department, Faculty of Engineering, Azarbaijan Shahid Madani  
University, P.O. BOX: 5375171379, Tabriz, Iran

### Syntheses

**Carboxylated carbon nanotubes (CNT-COOH).** Functionalization of MWCNTs was carried out via oxidation method with sonication of sulfuric acid (15 mL, 95–97 %) and nitric acid (45 mL, 65 %) having a ratio of 1:3 v/v for 6 h at 50 °C. A five-fold dilution was then applied to the mixture for stopping the oxidation reaction. Stirring and decantation were performed for five times and finally washed with deionized water by filtration until the water pH reached 7. The precipitate was finally dried in vacuum oven at 60 °C. The CNT-COOH with high oxidation was synthesized by the same procedure for 9 h at 60 °C.

**Thiophene functionalized carbon nanotubes (CNT-*f*-COOTh).** The 2-hydroxymethyl thiophene (CNT-COOH-*f*-HMTh) macroinitiator was synthesized by the esterification of

---

<sup>1</sup> Corresponding author (E-mail address): cnzhangguanghua@163.com

<sup>2</sup> Corresponding author (E-mail address): s.agbolaghi@azaruniv.ac.ir

CNT-COOH with 2-hydroxymethyl thiophene in the presence of para-toluene sulfonic acid (*p*-TSA) as a dehydrating agent (5 wt% of acid). A reactor was charged with CNT-COOH (0.5 g), 2-hydroxymethyl thiophene (1 g), and anhydrous dimethyl sulfoxide (50 mL), and then was sonicated with a bath type sonicator for 40 min to produce a homogeneous suspension. A catalytic amount of *p*-TSA was added to the reactor as a dehydrating agent and the reaction mixture was de-aerated by argon bubbling for 10 min. Thereafter, the flask was placed in a silicon oil bath at 140 °C and the reaction mixture was stirred for 6 h under argon atmosphere. The suspension was then centrifuged and washed several times with methanol for remove of remaining 2-hydroxymethyl thiophene. The CNT-COOH-*f*-HMTh powder was obtained after drying in reduced pressure at 55 °C. The CNT-COOH-*f*-HMTh macromonomer with a high density of thiophenic adducts was also prepared by the same procedure and with appropriate amounts of CNT-COOH (high density) (0.5 g) and 2-hydroxymethyl thiophene (2 g).

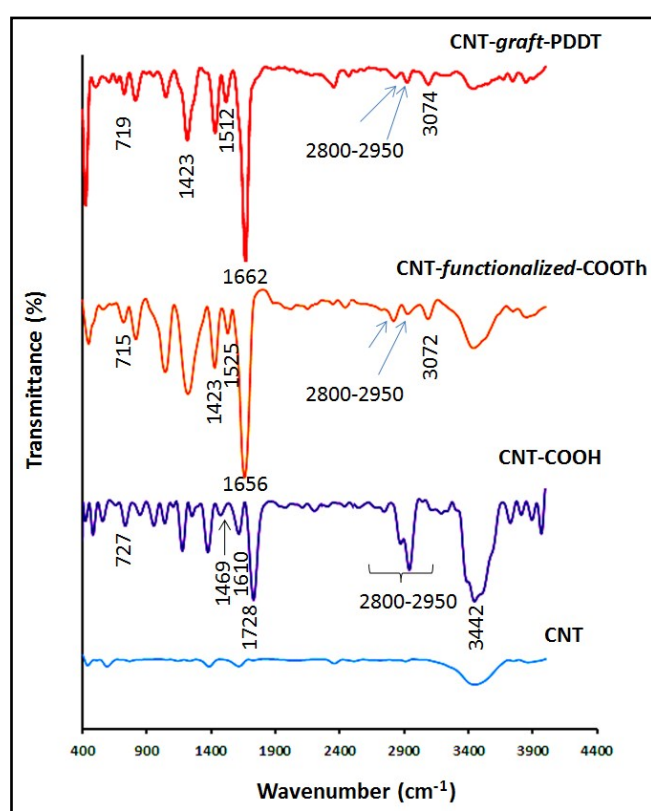
***Chemical oxidative graft polymerization of 3-dodecylthiophene from multi-walled carbon nanotubes (CNT-g-PDDT).*** A reactor was charged with CNTs-COOH-*f*-HMTh (0.5 g) and dried CHCl<sub>3</sub> (30 mL), and then was sonicated with a bath type sonicator for 40 min to reach a homogeneous suspension. Hereafter, 3-dodecylthiophene monomer (1.5 g) was added and the reaction mixture was deaerated by bubbling highly pure argon for 5 min. In a parallel system, 5 g of anhydrous ferric chloride was dissolved in 20 mL of dried acetonitrile. This solution was also deaerated and then slowly added to the reaction mixture at a rate of 5 mL min<sup>-1</sup> under an argon atmosphere. The reaction mixture was refluxed for 24 h at room temperature. The reaction was terminated by pouring the flask content into methanol. The product was filtered and washed several times with methanol. The dark color solid was dried in vacuum at room temperature. The crude product was extracted with CHCl<sub>3</sub> in Soxhlet for 24 h to remove pure poly(3-dodecyl thiophene). The polymer solution was filtered, precipitated into

excess methanol, and dried in reduced pressure to reach a dark color powder. The CNTs-g-PDDT possessing a high density of grafted thiophene (HD GCNT) was synthesized by the same method but with appropriate amounts of HD CNTs-COOH-*f*-HMTh (0.5 g), 3-dodecylthiophene monomer (3 g), and anhydrous ferric chloride (10 g).

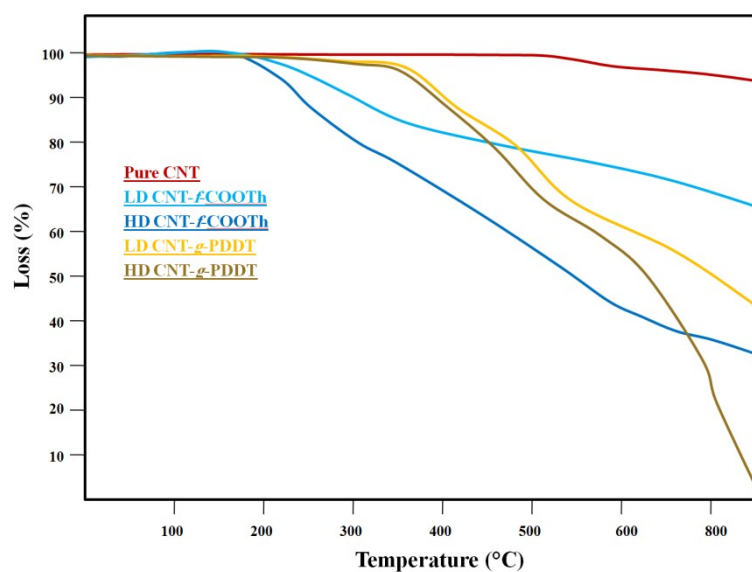
**Fourier transform infrared.** FT-IR spectrum of MWCNTs, carboxylated carbon nanotubes, and thiophene functionalized/grafted carbon nanotubes are reported in Fig. S1(a). In FT-IR spectrum of CNT-COOH, the stretching vibration absorbance of C=O in carboxylic acid appeared at  $1728\text{ cm}^{-1}$  and a broad peak centered at  $3442\text{ cm}^{-1}$  was detected as characteristic of an O-H stretch due to alcoholic or phenolic or carboxylic groups (Fig. S1(a)). In FT-IR spectrum of the thiophene functionalized carbon nanotubes, the vibrational peaks originating from the stretching of C-S and C=O were observed at around  $715$  and  $1656\text{ cm}^{-1}$ , respectively. The most important bands in FT-IR spectrum of CNT-g-PDDT were the weak aromatic  $\alpha$  and  $\beta$  hydrogens of thiophene rings at  $3000\text{--}3100\text{ cm}^{-1}$ ,  $\gamma(\text{C-H})$  in the aromatic ring at  $719\text{ cm}^{-1}$ , the aromatic C=C stretching vibration at  $1423, 1512\text{ cm}^{-1}$  and C-S stretching vibration in thiophene rings at  $702\text{ cm}^{-1}$ . Further vibration from the CH-aliphatic bonds could be detected at around  $2800\text{--}2950\text{ cm}^{-1}$ . FT-IR spectra assignments verified that the MWCNTs had been successfully oxidized into the shorter carboxylated carbon nanotubes (CNT-COOH) and after which, thiophene groups were successfully introduced into the carbon nanotubes (CNT-*f*-COOTh). After graft polymerization of thiophene derivatives onto functionalized CNTs, an increase was observed in the intensity of bands related to the polythiophene derivatives; however, the intensity of peaks attributed to MWCNTs decreased due to their low concentration in the grafted hybrid.

**Thermogravimetric analyses.** Fig. S1(b) represents thermogravimetric analyses (TGA) of the pure CNT, CNT-*f*-COOTh, and LD/HD CNT-g-PDDT samples. The pure CNTs commenced to decompose at about  $500\text{ }^{\circ}\text{C}$ , and the residue was 96 wt% at  $800\text{ }^{\circ}\text{C}$ . Hence, the pure CNTs

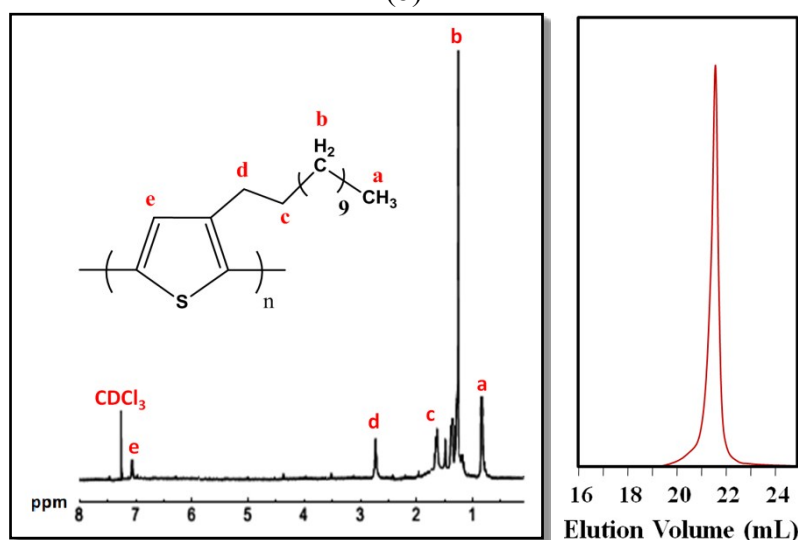
were stable and did not illustrate any dramatic decomposition in the range of 50–800 °C. On the contrary, the thermal decomposition of CNT-*f*-COOH began at 160 °C and the weight loss enhanced up to 800 °C with the residue value of 34 wt% for the CNT-*f*-COOH samples, respectively. Furthermore, the thermal decomposition of CNT-*g*-PDDT (Fig. S1(b)) started at 360 °C and the weight loss conspicuously increased up to about 530 °C, and thereafter the loss rate was decelerated. Moreover, <sup>1</sup>HNMR spectrum and SEC trace of PDDT oligomers are also represented in Figs. S1(c) and (d), respectively.



(a)



(b)



(c)

(d)

**Fig. S1.** FT-IR spectra of pure CNTs and respective functionalized and grafted derivatives (a); TGA curves of pure CNT as well as functionalized and grafted CNTs with thiophenic adducts (b); <sup>1</sup>H NMR spectrum (c) and SEC trace (d) of PDDT oligomer.

**Synthesis of PBDT-DTNT.** The 2,6-bis(trimethyltin)-4,8-di(2,3-didecylthiophen-5-yl)-benzo[1,2-b:4,5-b']dithiophene and 3,7-di(3-hexylthiophen-5-yl)-naphtho[1,2-c:5,6-c]bis[1,2,5]thiadiazole were added to dry toluene in a reactor under argon. Tris(dibenzylideneacetone)dipalladium(0) (Pd<sub>2</sub>(dba)<sub>3</sub>) as a catalyst and tri(*o*-tolyl)phosphine (P(*o*-tol)<sub>3</sub>) as a ligand were then quickly added to the reactor and the reaction mixture was

purged for 20 min. The reaction mixture was then heated to reflux for 48 h. Subsequently, the reactor was cooled to 30 °C and dropped into methanol. The resulted polymer was precipitated and collected by filtration. The PBDT-DTNT was obtained as a dark green solid. The number average molecular weight ( $M_n$ ) of synthesized polymer was 50 kDa and its polydispersity index (PDI) was 1.95. Fig. S2 represents  $^1\text{H}$ NMR spectra and size exclusion chromatography (SEC) trace of PBDT-DTNT. More details about the monomers synthesis are reported in the literature [1].  $^1\text{H}$ NMR (*ortho*-diclorobenzene (ODCB)- $d_4$ , 400 MHz),  $\delta$  (ppm): 8.78–8.82 (2 H), 8.11–8.13 (2 H), 7.87 (2 H) 7.38 (2 H), 2.43–2.76 (12 H), 1.04–1.60 (80 H), 0.65 (18 H).

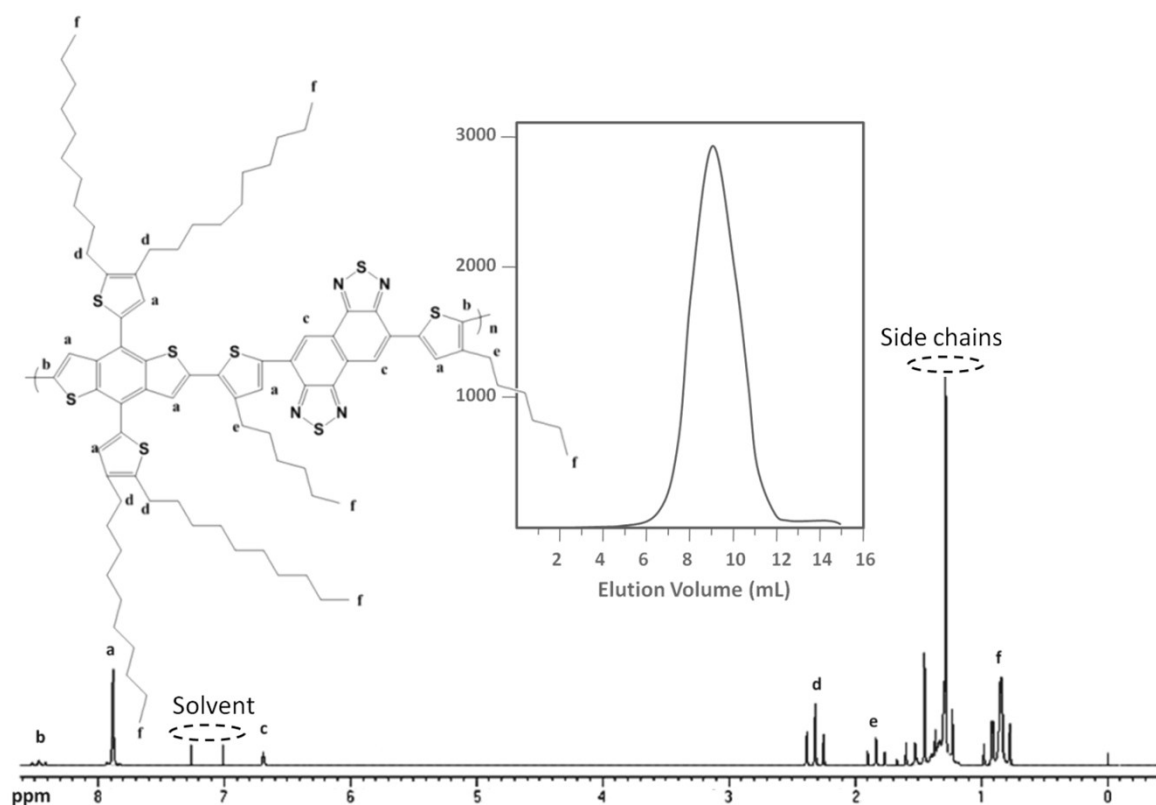


**Fig. S2.**  $^1\text{H}$ NMR spectra and SEC traces of synthesized PBDT-DTNT.

**Synthesis of CNT-g-PANI.** The carboxylic acid-functionalized CNT precursors (CNT-COOH) were prepared by sonication in the mixture of  $\text{H}_2\text{SO}_4$  and  $\text{HNO}_3$  (3:1, v/v) at 50 °C

within 12 h and then by centrifugation and washing with deionized water. To reach CNT-g-PANI [2], the aniline monomer was dissolved in ionic liquid, and CNT-COOH was dispersed in deionized water, which was followed by the addition of hydrochloric acid (1 M HCl) and potassium persulfate (KPS) (2:1 mol/mol). Through mixing these two solutions, an interface was formed between them. The PANI formed at the interface was then diffused into aqueous phase. The water phase was filled homogeneously with a dark-green CNT-g-PANI nanocomposite within 3 h. The aqueous phase was subsequently collected, washed, and dried at 40 °C for 24 h.

**Fourier transform infrared.** FT-IR spectra of pure CNT, CNT-COOH, and CNT-g-PANI are represented in Fig. S3(a). No principal peaks were detected for the pristine CNTs, as displayed at 500–3800  $\text{cm}^{-1}$  of Fig S3(a). FT-IR spectrum of CNT-COOH reflected a broad peak at 3442  $\text{cm}^{-1}$  for O–H stretch from carboxyl groups (O=C–OH and C–OH) and 2360  $\text{cm}^{-1}$  for O–H stretch from hydrogen-bonded –COOH. Furthermore, the C=C stretching was detected at 1634  $\text{cm}^{-1}$ , whereas the C=O and C–O stretching peaks were represented at 1730 and 1123  $\text{cm}^{-1}$ , respectively. The CNT-g-PANI demonstrated the stretching vibration bands at 1565  $\text{cm}^{-1}$  for the quinoid rings of C=C, 1493  $\text{cm}^{-1}$  for the benzenoid rings of C=C, 1288  $\text{cm}^{-1}$  for C–N and 1092  $\text{cm}^{-1}$  for C–H. These results proved that the surface of CNT was wrapped with PANI precursors and the core (CNT)-mantle (PANI) nano-hybrids were developed. Fig. S3(a) illustrates all peaks in question.

**Thermogravimetric analysis.** The TGA were carried out under a nitrogen atmosphere and the results are released in Fig. S3(b) for the pure CNT, CNT-COOH, and CNT-g-PANI. The weight reductions of CNTs observed at below 100 °C and between 150 and 300 °C were detected because of degradation of absorbed water and oxygen functional groups, respectively. For CNT-g-PANI, the degradation below 280 °C was correlated with the evaporation of absorbed solvent and decomposition of oxygen groups on CNT surface. The

weight losses at about 300 °C before 600 °C were occurred because of degradation and decomposition of PANI.

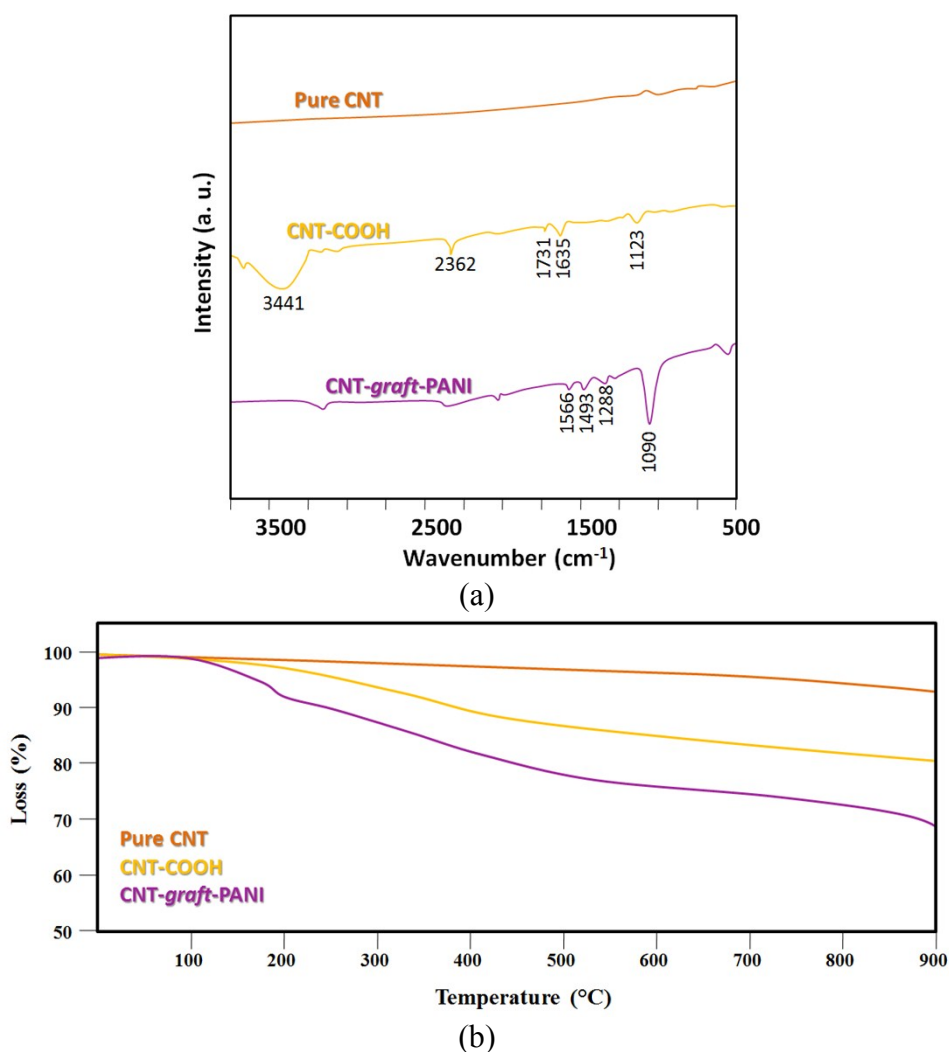


**Fig. S3.** FT-IR spectra (a) and TGA curves (b) of pure CNT, CNT-COOH, and CNT-g-PANI.

**Cyclic voltammetry.** The electrochemical experiments were conducted on Auto-Lab PGSTA T302N. Platinum foil and a saturated calomel electrode were used as the counter and reference electrodes, respectively. The working electrodes were fabricated by mixing the as-prepared powder with acetylene black and polytetrafluorene-ethylene (PTFE) binder and pressed onto nickel foam current-collectors. The measurements were carried out in a 1 M

KOH aqueous electrolyte at room temperature. Fig. S4 illustrates the cyclic voltammograms of CNT-COOH and CNT-g-PANI samples recorded in 1 M KOH.

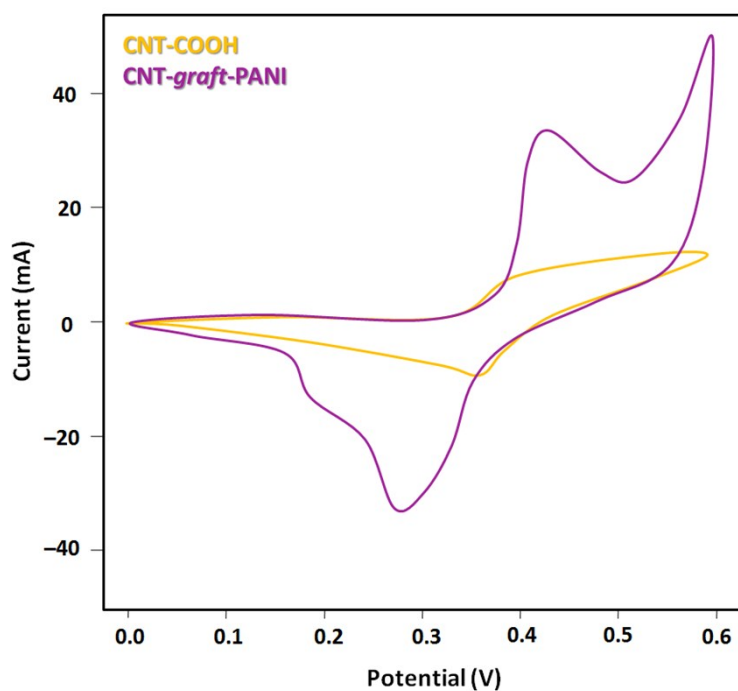


**Fig. S4.** Cyclic voltammograms of CNT-COOH and CNT-g-PANI recorded in 1 M KOH.

**X-ray photoelectron spectroscopy.** The XPS spectra of the N 1s core level (right panel in Fig. S5) for CNT-g-PANI composed of three subpeaks centered at 401.0 eV ( $-N=$ ), 402.2 eV ( $-NH-$ ), and 404.3 eV ( $-N+-$ ). These binding energy peaks could be correlated with the protonated amine units. The C 1s spectrum of CNT-g-PANI is also reported in Fig. S5(left). The peaks at 286.1, 287.5, 289.1 and 289.8 eV were assigned to C-C in aromatic ring, C-N, C-O and O-C=O bonds, respectively.

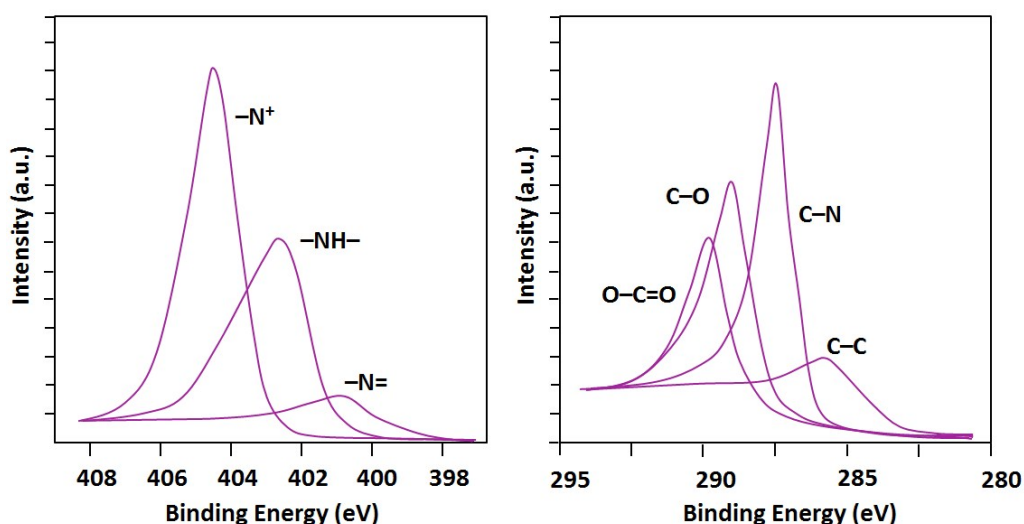


**Fig. S5.** XPS spectra of CNT-g-PANI prepared in HCl medium at core-levels of C 1s (left) and N 1s (right).

**Wide angle X-ray diffraction.** The wide angle X-ray diffraction (WAXD) patterns of pure CNT, CNT-*graft*-PANI, and CNT-*graft*-PANI/PBDT-DTNT are displayed in Fig. S6(a). The CNT spectrum represented a strong peak at  $2\theta = 26.4^\circ$ . The planes of (100), (211), and (020) were proved by appearance of  $2\theta$  peaks in  $21.40^\circ$ ,  $29.67^\circ$ , and  $30.95^\circ$ , respectively. In addition, the principal peaks of PBDT-DTNT crystals ranged at  $3.50\text{--}3.75^\circ$  (Fig. S6(a)). The insignificant peaks at  $4.5$ ,  $4.8$ ,  $5.3$  and  $6.2^\circ$  were also detected for the CNT-*graft*-PANI/PBDT-DTNT supramolecules.

**Ultraviolet-visible spectroscopy.** UV-Vis spectra of thin films prepared by core-mantle (CNT-*graft*-PANI) and core-mantle-shell (CNT-*graft*-PANI/PBDT-DTNT) nanostructures are exhibited in Fig. S6(b). The two peaks of 215 and 284 nm were detected for CNT-*graft*-PANI thin film due to  $\pi$ -interactions between the PANI chains and CNTs in the sample [3]. The peak at 382 nm indicated that PANI is protonated in the synthesized composite [4]. Furthermore, the maximum absorption wavelengths ( $\lambda_{\text{max}}$ ) for the PBDT-DTNT based nano-hybrids (core-mantle-shell CNT-*graft*-PANI/PBDT-DTNT nanostructures) were 449, 642,

and 680 nm [5]. The principal peaks for the interactions of CNT and PANI precursors were also observed at 220, 281, and 387 nm for the CNT-*graft*-PANI/PBDT-DTNT thin film [3,4].

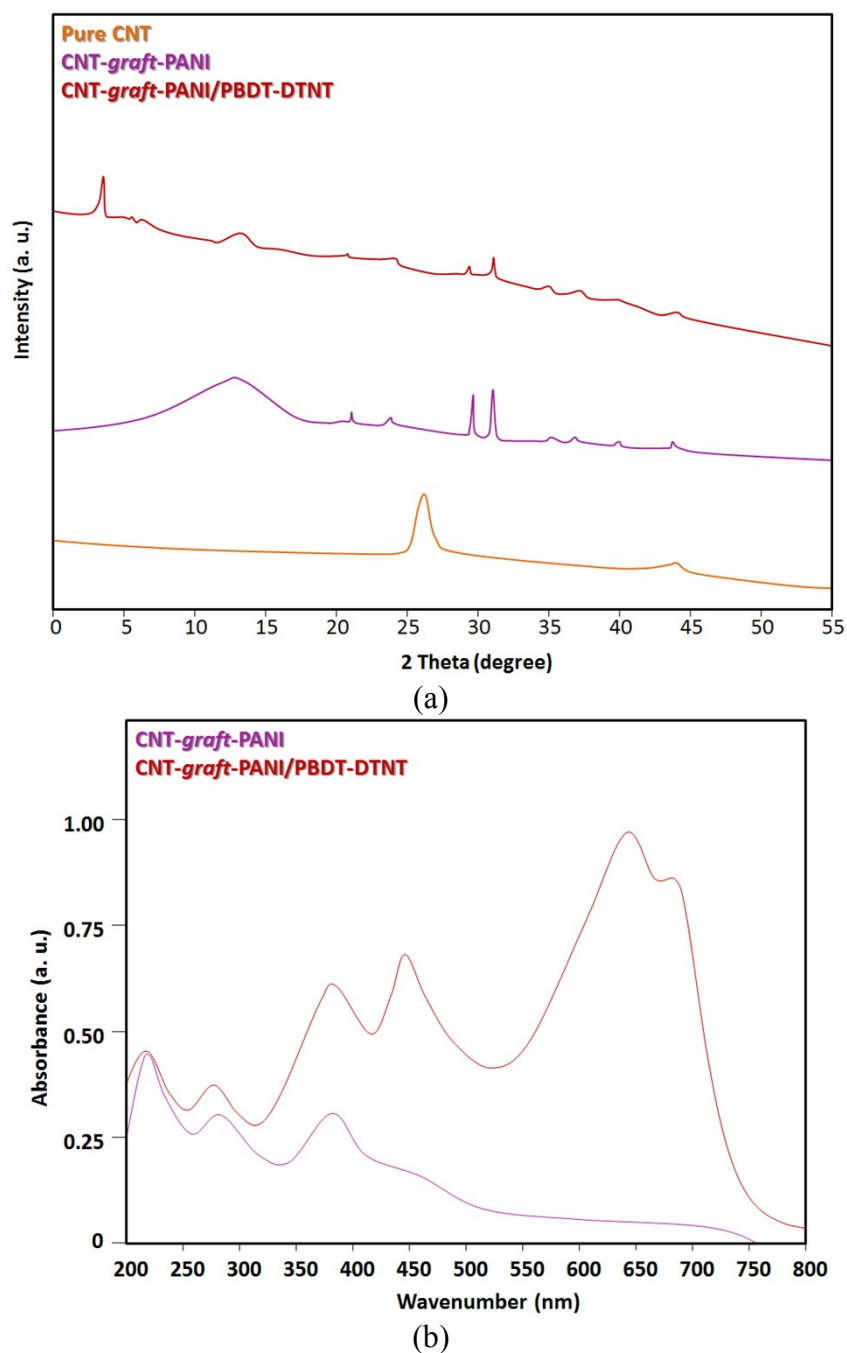


**Fig. S6.** (a) WAXD patterns of pure CNT, CNT-*g*-PANI, and CNT-*g*-PANI/PDDT-DTNT samples; (b) UV-Vis spectra of thin films prepared by CNT-*g*-PANI and CNT-*g*-PANI/PDDT-DTNT.

## References

- [1] Wang, M., Hu, X., Liu, P., Li, W., Gong, X., Huang, F. and Cao, Y., 2011. Donor–acceptor conjugated polymer based on naphtho [1, 2-c: 5, 6-c] bis [1, 2, 5] thiadiazole for high-performance polymer solar cells. *Journal of the American Chemical Society*, 133(25), pp.9638-9641.
- [2] Nguyen, V. H., Tang, L. and Shim, J.J., 2013. Electrochemical property of graphene oxide/polyaniline composite prepared by in situ interfacial polymerization. *Colloid and Polymer Science*, 291(9), pp.2237-2243.
- [3] Nguyen, V.H. and Shim, J.J., 2015. Green synthesis and characterization of carbon nanotubes/polyaniline nanocomposites. *Journal of Spectroscopy*, DOI:10.1155/2015/297804 (2015).
- [4] Stejskal, J., Kratochvil, P. and Radhakrishnan, N., 1993. Polyaniline dispersions 2. UV—Vis absorption spectra. *Synthetic Metals*, 61(3), pp.225-231.
- [5] Aghapour, S., Agbolaghi, S., Charoughchi, S., Sarvari, R. and Abbasi, F., 2019. Novel conjugated patterns of PBDT-DTNT and PBDT-TIPS-DTNT-DT complicated polymers onto graphenic nanosheets. *Polymer International*, 68(1), pp.64-70.